Muğla Sıtkı Koçman Üniversitesi Tıp Dergisi 2017;4(2):17-23
Medical Journal of Mugla Sitki Kocman University 2017;4(2):17-23

Orijinal Makale/Original Article
Ilica et al.

A Targeted High-Resolution Axillary MRI to Detect Axillary Lymph Node Metastasis with ADC Values

Aksiller Lenf Nodu ADC Değerlerinin, Yüksek Rezolüsyonlu MR ile Metastatik Lenf Nodu Tespitinde Kullanımı

Ahmet Turan ILICA[1], Cem OREN[2], Nurcan ERCIKTI[3], Brian GOLDNER[4], Inanç GUVENC[5], Erkan OZTURK[6], Ali Fuat CİCEK[7], Gokhan OSMANOGLU[8], Semih GORGULU[6]

[1]Turkish General Staff , Section of Radiology, Clinic, Ankara/Turkey
[2]University of Chicago , Dept of Radiology, Chicago, Illinois /USA
[3]University of Health Sciences Dept of Anatomy, Gulhane Training and Research Hospital , Ankara/Turkey
[4]Oregon Health and Sciences University Dept of Radiology, , Portland/OR/USA
[5]Medical Park Hospitals, Radiology Section, Ankara/Turkey
[6]Private office of breast and endocrine surgery, Ankara/Turkey
[7]University of Health Sciences Gulhane Training and Research Hospital Dept of Pathology, Ankara/Turkey
[8]Integrated Health Campus, Medical Manager, Etlik/Ankara/ Turkey

Abstract

To evaluate the clinical utility of ADC values of axillary lymph nodes using high-resolution axillary MR. 18 women with invasive breast carcinoma underwent axillary MR with surface coils. Two radiologists determined the most suspicious axillary lymph node using predefined morphologic descriptors and measured the ADC values of the most suspicious lymph node in consensus. Statistical analysis was performed to evaluate the diagnostic value of ADC measurements using the pathologic assessment as the reference study. Histopathologic findings revealed axillary nodal metastases in 11 out of 18 patients. ADC values of metastatic lymph nodes were lower than the nonmetastatic nodes (p=0.006, Mann Whitney U test). By using 0.967×10^{-3} mm^2/s as a threshold, sensitivity, specificity, accuracy, positive predictive value, and negative predictive values based for ADC were 85.7, 100.0, 94.4, 91.7, 100.0. If our initial results are confirmed with larger series, ADC values of the axillary lymph nodes with high-resolution axillary MRI can be an alternative for sentinel lymph node biopsy.

Keywords: Apparent Diffusion Coefficient, Axillary Lymph Node, Breast Cancer, Diffusion MRI

Öz

Yüksek rezolüsyonlu MR ile ölçülen aksiller lenf nodu ADC değerlerinin klinik etkinliğinin araştırılması. İnvaziv meme kanserli 18 kadına yüzeyel koiller ile aksiller MR çekimi yapıldı. İki radyolog belirlenmiş morfolojik kriterlere göre malignite açısından en şüpheli aksiller lenf nodunu konsensus ile belirleyerek en şüpheli lenf nodunda ADC ölçümü yaptılar. Patolojik sonuçlar referans kabul edilerek ADC ölçümlerinin metastatik-reaktif lenf nodu ayrımında tanısal etkinliğini belirlemede gerekli istatistik değerlendimeler yapıldı. Histopatolojik bulgular 18 hastanın 11'inde aksiller lenf nodu metastazı saptadı. Metastatik lenf nodlarının ADC değerleri olmayanlardan daha düşüktü (p=0.006, Mann Whitney U testi). ADC değerli olarak 0.967×10^{-3} mm^2/s değeri eşik değer olarak kabul edildiğinde istatistiksel olarak duyarlılık, özgüllük, doğruluk, pozitif prediktif ve negatif prediktif değer sırasıyla 85.7, 100.0, 94.4, 91.7, 100.0 olarak belirlendi. Eğer bizim bu konudaki ilk bulgularımız daha geniş seriler ile desteklenirse yüksek rezolüsyonlu MR ile ölçülen aksiller lenf nodu ADC değerleri gelecekte sentinel lenf nodu biyopsisine iyi bir alternatif tarama metodu olabilir.

Anahtar Kelimeler: Aksiller Lenf Nodu, Difüzyon MR, Görünüşteki Difüzyon Katsayısı, Meme Kanseri

Introduction

Breast carcinoma is the most common malignancy among women (1). Presence or absence of axillary lymph node (ALN) metastases at the time of diagnosis have a significant impact on the overall prognosis as well as the therapeutic approach (2-4) since patients with nodal involvement might benefit from preoperative adjuvant chemotherapy. Although axillary lymph node dissection (ALND) was previously the standard method of lymph node staging in breast cancer, it has been supplanted by sentinel lymph node biopsy (SLNB.) SLNB is a less-invasive procedure that is preferred in patients who are node negative based on clinical exam (5). However, SLNB has technical and conceptual limitations. It is a somewhat invasive technique that is associated with significant morbidity, such as

lymphedema, although this is less of a risk than ALND. False-negative results can occur in up to 15% of patients (6-8). Most of these false-negative results occur due to massive lymph node metastasis in the first drainage node (6).

Many techniques of risk stratification have been evaluated, such as ultrasound (US), and computed tomography (CT) in order to reduce the number of patients undergoing unnecessary SLNB or a second axillary procedure. Unfortunately, these studies showed poor sensitivity and specificity (9-15).

MR is increasingly being used in patients with breast cancer and has become a standard imaging tool for pretherapeutic staging of breast cancer (16-28). However, use of MR for the evaluation of axillary lymph nodes has remained limited. This is mostly due to inclusion of the axillary region to, which is limited by the contours seen with a standard breast coil. Therefore, a non-invasive imaging technique that allows accurate preoperative assessment of the ALNs reliably becomes of utmost importance.

Muğla Sıtkı Koçman Üniversitesi Tıp Dergisi 2017;4(2):17-23
Medical Journal of Muğla Sitki Kocman University 2017;4(2):17-23

Orijinal Makale/Original Article
Ilica et al.

In this prospective study, we aimed to test a targeted high-resolution MR protocol for imaging of the axillary region. We assessed the diagnostic accuracy of ADC values in differentiating nodal positive from nodal negative breast cancers.

Material and Method

Patient Selection

This prospective study was approved by the institutional review board, and the requirement to obtain informed consent was waived. The study population initially included 34 patients. The inclusion criteria for this study were: 1) patients with histopathologically confirmed breast carcinoma; 2) patients planning to undergo mastectomies and ALND with en bloc resection of axillary lymph nodes on the ipsilateral side within 3 days after axillary MR examination. Patients with cancer recurrence and secondary breast cancer were not eligible for this study. Fifteen women, who did not undergo either SLNB or ALND or who had a substantial delay between axillary MR and surgical staging, were excluded from the study. One patient was excluded due to poor image quality from motion artifact. The remaining 18 women (age range, 40-75 years, mean age 55.8 years) with invasive breast carcinoma were recruited. All patients underwent a targeted preoperative axillary MR protocol at 3 T between July 2010 and July 2011.

Imaging Methods
Axillary MR Protocol

MR exams were performed in 3 days before surgery in all patients. Patients were scanned using a 3-T MR scanner (Philips Achieva. Best, Netherlands.) A multichannel phased-array, flex, large surface coil was placed over the axilla with the patient in the prone position with her arm elevated above her head (Figs. 1a and 1b).To assess ALN status, three sequences were acquired in axial orientation. The field of view of all three sequences was optimized to cover all locoregional levels. The MR protocol included axial T1-weighted turbo spin-echo; axial T2-weighted turbo spin-echo and axial diffusion-weighted MR imaging with 3 b values (0, 500, 1000 s/mm^2) .

Parameters of T1W axial MR images were as follows: turbo spin echo (TSE), repetition time/echo time 534/10 ms; Bandwidth (Hz) 218.8; flip angle 90; NSA (number of sıgnal avarage) 1; section thickness 3 mm; interval 0.3 mm; field of view (FOV) 200x200x115mm; matrix 512x224X169; number of excitations 1; 35 slices; total time of acquisition 2 min 43 s.

Parameters of T2W axial MR images were as follows: turbo spin echo (TSE), repetition time/echo time, 3505/120 ms; Bandwidth (Hz) 217.3; flip angle, 90; NSA:1, section thickness, 3 mm; interval, 0.3; FOV 200x200x115mm; matrix, 432x268X192;

number of excitations,1; 35 slices; total time of acquisition 1 min 34 s.

DWI was performed using the following parameters: SE-EPI single-shot sequence; TR/TE 2264/58 msec, Bandwidth (Hz) 19.3; FOV 200x200x115 mm; NSA: 3, slice thickness 3 mm; an intersection gap of 0.3 mm; 320x92X105 matrix, b-values of 0,500,1000 s/mm^2, MPG pulses in the x-, y-, and z-axes, total time of acquisition 5 min 02 s. Breath-holding, respiratory triggering, and parallel imaging were used.

Total examination time for all dedicated protocol was 9 minutes 18 s.
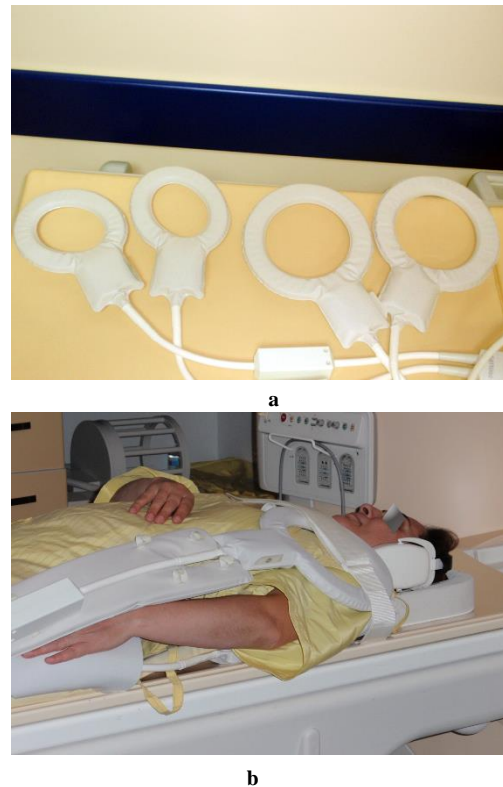
Figure 1. Photograph of large and small surface coils (a). The large surface coil is seen positioned close to patient's axilla (b).

Image Analysis

A consensus reading was performed between pathologist, surgeons, and radiologist to assess the most suspicious lymph node chosen by MRI. The features including the level, shape and depth of the most suspicious lymph node on MRI was used by surgeon to provide the most accurate assignment between MRI and histopathology. Besides knowledge of the diagnosis of breast cancer no other clinical or imaging data were known by the radiologists. Loss of fatty hilum, round and less reniform shape, concentric or eccentric cortical thickening, irregular contours, blurring of perinodal fat, necrosis, capsulary effraction were accepted as signs that suggest metastatic lymph node involvement as reported in previous studies (26-31).

Muğla Sıtkı Koçman Üniversitesi Tıp Dergisi 2017;4(2):17-23
Medical Journal of Muğla Sitki Kocman University 2017;4(2):17-23

Orijinal Makale/Original Article
Ilica et al.

Both readers chose the most suspicious axillary lymph node for metastasis on the basis of these morphologic criteria on axial T1-weighted and T2-weighted images in consensus. In the second step, the same most suspected ALN on the DW images was identified by slice by slice comparison with conventional MR images. For quantitative assessment, ADC measurements were made by the same two readers in consensus by placing a freehand circular or elliptical region of interest (ROI) over the suspected ALN. The ROI was carefully placed over the cortex so as to avoid the periphery of the ALN due to concerns about volume averaging. A mean of three values was recorded for all suspected ALN. The median ADC values derived from the signal intensity averaged across images obtained with b values of 0, 500, and 1000 sec/mm^2 were then calculated for each ALN from all patients. Results of the ADC values in the most suspected ALN of metastatic and nonmetastatic patients were compared with the overall lymph node status (i.e., nodal status positive or nodal status negative).

Radioisotope scintigraphy

Scintigraphy was performed the day prior to breast surgery. Technetium 99 m-labeled tin colloid was injected intradermally above the cancer and peritumorally, and lymphoscintigraphy was conducted 4 hours later. A set of planar images was obtained. The sentinel lymph node (SLN) was localized by the detection of radioactivity. In this study, the ipsilateral axillary SLN could be detected in all patients.

Surgical Procedure, Reference standard

In case of positive sentinel lymph nodes, ALND including level 1 and 2 was performed. Targeted axillary lymph nodes were carefully removed according to the MR images and labeled for location and orientation. Lymph nodes obtained at SLNB and ALND were examined by using standard hematoxylin and eosin stained sections (31). Final surgical histopathologic findings in all metastatic patients were defined as the reference standard for axillary nodal staging. For nonmetastatic patients, who had negative SLNB, negative axillary MRI and negative axillary US results, 2 year follow up was defined as the reference standard for axillary nodal staging. Sensitivity, specificity, positive predictive value, and accuracy were calculated for ADC values.

Statistical analysis

Statistical analysis was performed using SPSS v15.0 for Windows. Descriptive statistics were expressed as frequency tables and cross tables for categorical variables and presented as median, minimum, and maximum for numerical variables. Mann-Whitney U test was used in two group comparisons of numeric variables that were non-normally distributed. In order to determine cut-off values, Roc-curve analysis was performed. Statistical significance level was set at p<0.05.

Results

Thirteen patients were found to have invasive ductal carcinoma, 3 had invasive lobular carcinoma, 1 with invasive papillary carcinoma, and 1 mixed ductal/lobular carcinoma after the pathological review. For the longest diameters, ALN sizes differed between 8 mm and 24 mm. For the shortest diameters, ALN sizes differed between 6 mm and 13 mm. Final surgical histopathologic findings at ALND revealed axillary nodal metastases in 11 out of 18 patients. Median ADC values of metastatic lymph nodes [0.83 (0.43-0.94) (x10^{-3})] were found to be lower than the normal lymph nodes [1.30 (0.75-1.68) x10^{-3})] shown in Table 1 and Figs. 2, 3 and 4. Only 1/11 metastatic lymph nodes showed neither of the morphologic features stated above. By using 0.967 x10^{-3} mm^2/s as a threshold , sensitivity, specificity, accuracy, positive predictive value and negative predictive values based on ADC values were 85.7,100.0, 94.4, 91.7, 100.0, respectively (Table 4). Tables 2 and 3 shows different ADC cutoff values and distributions between lymph nodes in patients found to have metastatic disease at ALN and those without.

Table 1. Summary of ADC measurements

	Total ALNs (n=18)	Metastatic ALNs (n=11)	Nonmetastatic ALNs (n=7)	p
Median (min-max) ADC x10^{-3}	0.89 (0.43-1.68)	0.83 (0.43-0.94)	1.30 (0.75-1.68)	0.006

ALNs: Axillary lymph nodes, ADC: Apparent diffusion coefficient

Table 2. Prediction of axillary status based on the cutoff ADC value of 0.95x x10^{-3} (0.95)

		Cutoff 0.95
ADC value	Sensitivity	85.7
	Specificity	100.0
	Accuracy	94.4
	Positive predictive value	91.7
	Negative predictive value	100.0

Table 3. Distribution of axillary status according to different cut-off ADC (Apparent diffusion coefficient) values

		Metastatic (n=11)	Nonmetastatic (n=7)
ADC value	<0.9	8	1
	≥0.9	3	6
	<0.95	11	1
	≥0.95	0	6
	<1	11	2
	≥1	0	5

Muğla Sıtkı Koçman Üniversitesi Tıp Dergisi 2017;4(2):17-23
Medical Journal of Muğla Sitki Kocman University 2017;4(2):17-23

Orijinal Makale/Original Article
Ilica et al.

Table 4. ROC analysis of ADC values

If ≥ x 10^{-3} mm^2/s	Average ADC Sensitivity	1-Specificity
0.428	1.000	1.000
0.541	1.000	0.909
0.693	1.000	0.818
0.739	1,000	0.727
0.773	0.857	0.727
0.812	0.857	0.636
0.830	0.857	0.545
0.848	0.857	0.455
0.865	0.857	0.364
0.886	0.857	0.273
0.908	0.857	0.182
0.925	0.857	0.091
0.967	0.857	0.000
1.099	0.714	0.000
1.252	0.571	0.000
1.312	0.429	0.000
1.377	0.286	0.000

Discussion

Criteria based on size and morphology of ALN on MRI may improve detecting axillary metastasis, however, MRI results based on morphological features may be inaccurate in the metastatic ALNs with normal size and shape (16-22). These limitations emphasize the importance of functional imaging. DW MRI, which is highly sensitive to tissue microstructure, seems to be a suitable functional imaging technique, and it has been observed that the apparent diffusion coefficient (ADC) values are significantly reduced in primary or secondary cancer tissues. Although DWI MRI is the standard protocol for breast cancer evaluation, its efficacy in the assessment of axillary region is limited due to inadequate coverage of axillary region, low spatial resolution and susceptibility artifacts. Visualization of the axillary region was only achievable using a standard receive-only bilateral breast coil encompassing both breasts and axilla but at the expense of non-uniform images and partial coverage of the axilla. All of the published data on DW MRI characteristics of axillary lymph nodes was performed with standard breast coils and were done as a part of routine breast MRI protocol (25-28). We developed a dedicated axillary MRI by using surface coils rather than standard breast coils to achieve a high-spatial-resolution. We were able to obtain high-resolution images of axillary regions by using a dedicated MR examination with several surface coils. This improved the accuracy of ADC measurements on MR DWI of axilla with a magnetic field strength of 3-T with multichannel capability in


a

b

c
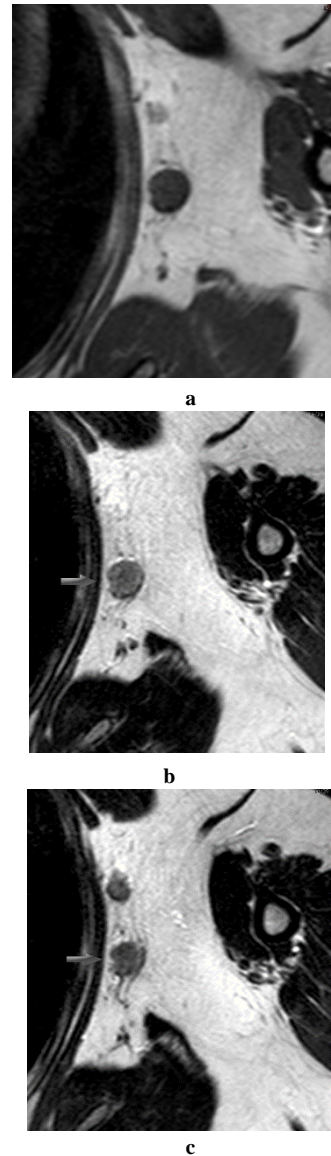
Figure 2. The 39 year-old woman with grade 2 infiltrating ductal carcinoma (stage IIIB) and positive pathologic findings from axillary lymph node dissection. Unenhanced axial T1(a) and T2(b) weighted images shows a round axillary node (arrow) with thick concentric cortex and absent central fatty hilum. Axial T2 weighted image (c) in another patient shows malignant axillary nodes with irregular contours (arrow)

our study. The flexibility and different available sizes of the surface coils allowed adequate exposure of the axilla with the closest possible contact between the skin and the coil, which is not achieved with a standard breast coil.

Moreover, an inherent advantage of our technique was that the visualization of small nodes is not altered, even in deeply located nodes, which is not the case with sonography (32,33). We were able to identify subtle morphologic features suggesting metastatic disease. Minimal asymmetric cortical thickenings, subtle cortical irregularities and even perinodal fat infiltration and perivascular nodal invasion were some of the features we identified in

Muğla Sıtkı Koçman Üniversitesi Tıp Dergisi 2017;4(2):17-23
Medical Journal of Mugla Sitki Kocman University 2017;4(2):17-23

Orijinal Makale/Original Article
Ilica et al.

these patients that were not observed with conventional MRI exam because of insufficient spatial resolution with standard breast coils. Further characterization of these morphologic features seen on high resolution MRI is among our aims in the near future.

a

b

c
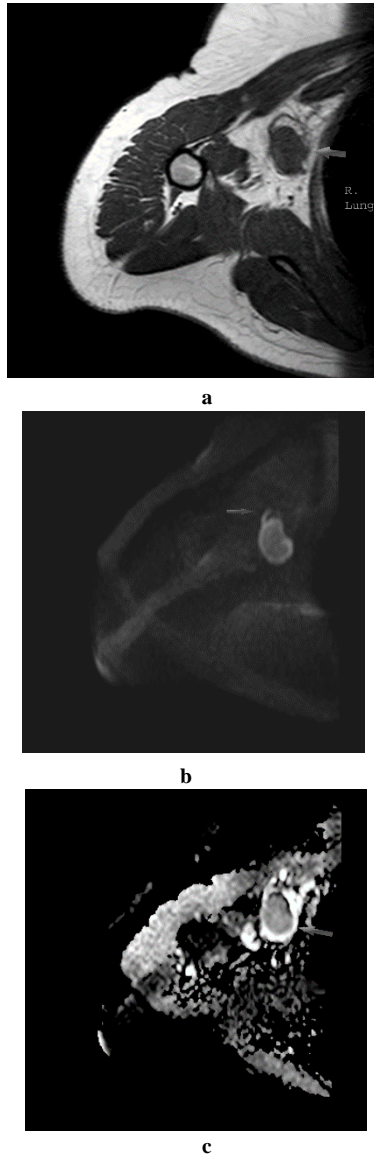
Figure 3. The 62 year-old woman with infiltrating ductal carcinoma (T2N2M0: Stage III A). Unenhanced axial T1 weighted image (a) shows a large oval lymph node with irregular borders. An axial DW MR image (b) obtained with b-1000 shows hyperintense lymph node. Hyperinsensity is seen extending along the vascular structure suggesting extracapsular vascular invasion(arrow). Corresponding ADC map image (c) confirms the metastatic nature of the lymyp node by showing dark signal (ADC value: 0.78 x10⁻³)

The results of the present study showed that the ADC value of metastatic ALNs was significantly lower than that of nonmetastatic ALNs. This result was concordant with nearly all previous recent studies (22,34-40). The lower ADC values may be due to high cellularity within the metastatic ALN. The ADC values reported for metastatic ALN ranged

from 0.666 to 1.369 in the literature (22,34-40). All of the metastatic ALNs had ADC values lower than $1 \times (x10^{-3})$ in our study. While false-negative results for SLNB was reported in up to 15% of patients (6-8), there was no false negative ALN in our study.

a

b

c
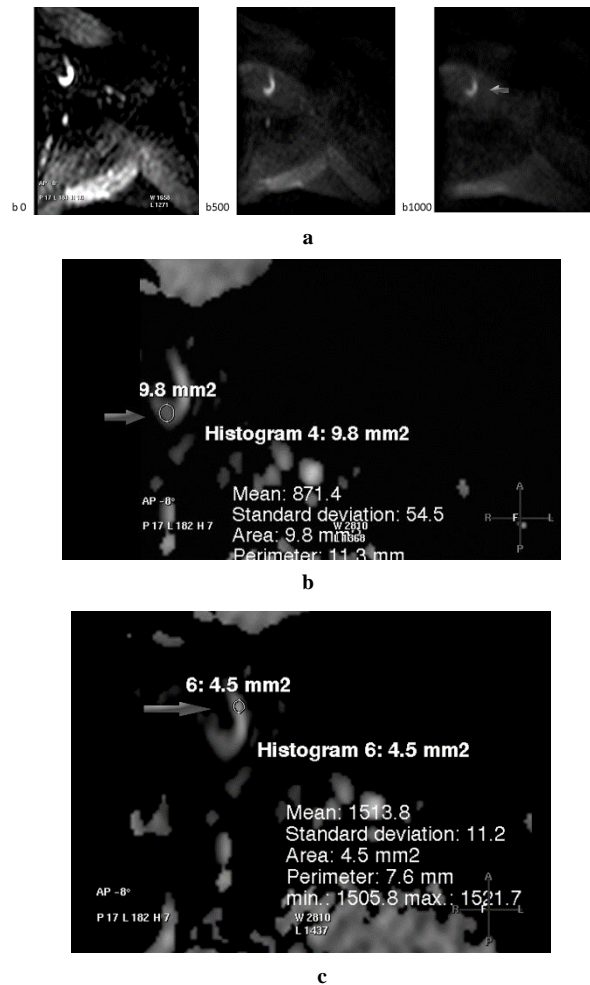
Figure 4. The 59 year-old woman with grade 2 infiltrating ductal carcinoma of the left breast. (T1N1M0: Stage IIA). Metastatic lymp node localized in the posterior cortex of lymp node. There is a persistent hiperintensity within the posterior part of the lymph node in high b value (1000) MR image (a). Corresponding ADC image (b) shows dark signal within the posterior cortex of lymph node as compared to anterior part. ADC values measured within the posterior metastatic part shows lower ADC values (0.87 x10⁻³) c) ADC values measured within the anterior nonmetastatic part shows higher values (1.51x x10⁻³)). This case shows how ADC measurements can detect small intranodal metastases in a lymph node with a normal cortex thickness without any morphologic abnormality.

There was only 1 false positive ALN which had a ADC value is lower than $0.89 \times (x10^{-3})$. This may be due to distorted image quality or sampling error. All of the nonmetastatic ALN in our patients had ADC values higher than $0.9 \times (x10^{-3})$ except 1 case, which was the only false positive result. There are a few others who reported conflicting results showing higher ADC values for metastatic ALN (41,42). We believe that those conflicting results arise from

incorrect sampling within the ALN. Our study showed that metastatic involvement of ALN may affect some portion of ALN without changing its normal reniform shape. Involving the whole ALN to the ADC measurement may cause higher ADC values which does not reflect the true ADC value of the metastatic ALN. A necrotic part of an ALN or an inflammation due to edema within the ALN may be avoided from ADC sampling with the help of a high b value DW MRI sequence obtained in a dedicated axillary MRI exam. Morphological features of ALN can not be appreciated with a routine breast MRI and can cause incorrect sampling of the ALN for ADC measurements.

Our study has a few limitations. First, only a small number of patients were included. In order to achieve an exact correlation between MRI-identified ALN, and removed at dissection and analyzed at pathology, we chose the most suspicious ALN on MRI which was easier to label and correlate. This could not be systematically achieved for all lymph nodes , especially for nodes less than 3 mm. Unfortunately there is no well accepted physical reference within the en bloc resected axillary specimens that could used for the resected ALNs. Poor image quality due to respiration or other movement is a drawback of our protocol but still the image quality is much better than a standard breast MRI. This is more pronounced with patients with large body habitus. However, short scan times allowed technologists to easily repeat a poor quality sequence.

In conclusion, our initial results regarding the ADC values of the axillary lymph nodes which were obtained using a high-resolution axillary MRI for the purpose of detecting axillary nodal metastases are promising. If our initial results are confirmed with larger series in the near future, the axillary MRI can be considered as an alternative to SLN biopsy before initial breast cancer surgery.

References

1. Jemal A, Siegel R, Ward E, Hao Y, Xu J, Thun MJ. Cancer statistics. CA Cancer J Clin. 2009;59(4):225-49.
2. Singletary SE, Connolly JL. Breast cancer staging: working with the sixth edition of the AJCC Cancer Staging Manual. CA Cancer J Clin. 2006;56(1):37-47.
3. Crippa F, Gerali A, Alessi A, Agresti R, Bombardieri E. FDG-PET for axillary lymph node staging in primary breast cancer. Eur J Nucl Med Mol Imaging. 2004;31(Suppl 1):97-102.
4. Meinel LA, Abe H, Bergtholdt M, Ecanow J, Schmidt R, Newstead G. Multi-modality morphological correlation of axillary lymph nodes. Int J Comput Assist Radiol Surg. 2010; 5(4):343-50.
5. Reintgen D, Giuliano R, Cox CE. Sentinel node biopsy in breast cancer: an overview. Breast J. 2000;6(5):299-305.
6. Ahn JH, Son EJ, Kim JA, et al. The role of ultrasonography and FDG-PET in axillary lymph node staging of breast cancer. Acta Radiol. 2010;51(8):859-65.
7. Borqstein PJ, Pijpers R, Comans EF, van Diest PJ, Boom RP, Meijer S. Sentinel lymph node biopsy in breast cancer: guidelines and pitfalls of lymphoscintigraphy and gamma probe detection. J Am Coll Surg. 1998;186(3):275-83.
8. Chaqpar AB, Martin RC, Scoqqins CR, et al. Factors predicting failure to identify a sentinel lymph node in breast cancer. Surgery. 2005;138(1):56-63.
9. Baruah BP, Goyal A, Young P, Douglas-Jones AG, Mansel RE. Axillary node staging by ultrasonography and fine-needle aspiration cytology in patients with breast cancer. Br J Surg. 2010;97(5):680-3.
10. Lumachi F, Ferretti G, Povolato M, et al. Usefulness of 99m-Tc-sestamibi scintimammography in suspected breast cancer and in axillary lymph node metastases detection. Eur J Surg Oncol. 2001;27(3):256-9.
11. Uematsu T, Sano M, Homma K. In vitro high-resolution helical CT of small axillary lymph nodes in patients with breast cancer: correlation of CT and histology. AJR Am J Roentgenol. 2001;176(4):1069-74.
12. Murray AD, Staff RT, Redpath TW, et al. Dynamic contrast enhanced MRI of the axilla in women with breast cancer: comparison with pathology of excised nodes. Br J Radiol. 2002;75(891):220-8.
13. Wahl RL. Current status of PET in breast cancer imaging, staging, and therapy. Semin Roentgenol. 2001;36(3):250-60.
14. Yoshimura G, Sakurai T, Oura S, et al. Evaluation of axillary lymph node status in breast cancer with MRI. Breast Cancer. 1999;6(3):249-58.
15. Sachelarie I, Grossbard ML, Chadha M, Feldman S, Ghesani M, Blum RH. Primary systemic therapy of breast cancer. Oncologist. 2006;11(6):574-89.
16. Harada T, Tanigawa N, Matsuki M, Nohara T, Narabayashi I. Evaluation of lymph node metastases of breast cancer using ultrasmall superparamagnetic iron oxide-enhanced magnetic resonance imaging. Eur J Radiol. 2007;63(4):401-7.
17. Michel SC, Keller TM, Frohlich JM, et al. Preoperative breast cancer staging: MR imaging of the axilla with ultrasmall superparamagnetic iron oxide enhancement. Radiology. 2002;225(2):527-36.
18. Stets C, Brandt S, Wallis F, et al. Axillary lymph node metastases: a statistical analysis of various parameters in MRI with USPIO. J Magn Reson Imaging. 2002;16(1):60-8.
19. Dong H, Li Y, Yu K, Li H. Comparison of image quality and application values on different field-of-view diffusion-weighted imaging of breast cancer. Acta Radiol. 2016;57(1):19-24.
20. Tamura T, Murakami S, Naito K, Yamada T, Fujimoto T, Kikkawa T. Investigation of the optimal b-value to detect breast tumors with diffusion weighted imaging by 1.5-T MRI. Cancer Imaging. 2014;14:11
21. Çabuk G, Nass Duce M, Özgür A, Apaydın FD, Polat A, Orekici G. The diagnostic value of diffusion-weighted imaging and the apparent diffusion coefficient values in the differentiation of benign and malignant breast lesions. J Med Imaging Radiat Oncol. 2015;59(2):141-8.
22. Nakai G, Matsuki M, Harada T, et al. Evaluation of axillary lymph nodes by diffusion-weighted MRI using ultrasmall superparamagnetic iron oxide in patients with breast cancer: Initial clinical experience. J Magn Reson Imaging. 2011;34(3):557-62.
23. Bernd H, De Kerviler E, Gaillard S, Bonnemain B. Safety and tolerability of ultrasmall superparamagnetic iron oxide contrast agent: comprehensive analysis of a clinical development program. Invest Radiol. 2009;44(6):336-42.
24. Motomura K, Ishitobi M, Komoike Y, et al. SPIO-enhanced magnetic resonance imaging for the detection of metastases in sentinel nodes localized by computed tomography lymphography in patients with breast cancer. Ann Surg Oncol. 2011;18(12):3422-9.
25. Iima M, Le Bihan D, Okumura R, et al. Apparent diffusion coefficient as an MR imaging biomarker of low-risk ductal carcinoma in situ: a pilot study. Radiology. 2011;260(2):364-72.
26. Scaranelo AM, Eiada R, Jacks LM, Kulkarni SR, Crystal P. Accuracy of Unenhanced MR Imaging in the Detection of Axillary Lymph Node Metastasis: Study of Reproducibility and Reliability. Radiology. 2012;262(2):425-34.
27. Luciani A, Dao TH, Lapeyre M, et al. Simultaneous bilateral breast and high-resolution axillary MRI of patients with

breast cancer: preliminary results. AJR Am J Roentgenol. 2004;182(4):1059-67.

28. Baltzer PA, Dietzel M, Burmeister HP, et al. Application of MR mammography beyond local staging: is there a potential to accurately assess axillary lymph nodes? evaluation of an extended protocol in an initial prospective study. AJR Am J Roentgenol. 2011;196(5):641-7.

29. Kvistad KA, Rydland J, Smethurst HB, Lundgren S, Fjosne HE, Haraldseth O. Axillary lymph node metastases in breast cancer: preoperative detection with dynamic contrast-enhanced MRI. Eur Radiol. 2000;10(9):1464-71.

30. Mortellaro VE, Marshall J, Singer L, et al. Magnetic resonance imaging for axillary staging in patients with breast cancer. J Magn Reson Imaging. 2009;30(2):309-12.

31. Koelliker SL, Chung MA, Mainiero MB, Steinhoff MM, Cady B. Axillary lymph nodes: US-guided fine-needle aspiration for initial staging of breast cancer-correlation with primary tumor size. Radiology. 2008;246(1):81-9.

32. Luciani A, Dao TH, Lapeyre M, et al. Simultaneous bilateral breast and high-resolution axillary MRI of patients with breast cancer: preliminary results. AJR Am J Roentgenol. 2004;182(4):1059-67.

33. Vassallo P, Wernecke K, Roos N, Peters PE. Differentiation of benign from malignant superficial lymphadenopathy: the role of high-resolution US. Radiology. 1992;183(1):215-20.

34. Yamaguchi K, Schacht D, Nakazono T, Irie H, Abe H. Diffusion weighted images of metastatic as compared with nonmetastatic axillary lymph nodes in patients with newly diagnosed breast cancer. J Magn Reson Imaging. 2015;42(3):771-8.

35. Scaranelo AM, Eiada R, Jacks LM, Kulkarni SR, Crystal P. Accuracy of unenhanced MR imaging in the detection of

axillary lymph node metastasis: study of reproducibility and reliability. Radiology. 2012;262(2):425-34.

36. Fornasa F, Nesoti MV, Bovo C, Bonavina MG. Diffusion-weighted magnetic resonance imaging in the characterization of axillary lymph nodes in patients with breast cancer. J Magn Reson Imaging. 2012;36(4):858-64.

37. Kim EJ, Kim SH, Kang BJ, Choi BG, Song BJ, Choi JJ. Diagnostic value of breast MRI for predicting metastatic axillary lymph nodes in breast cancer patients: diffusion-weighted MRI and conventional MRI. Magn Reson Imaging. 2014;32(10):1230-6.

38. Miami L, Masako K. Ryosuke O, Kaori T. Detection of axillary lymph node metastasis with diffusion-weighted MR imaging. Clin Imaging. 2014;38(5):633-6.

39. Schipper RJ, Paiman ML, Beets-Tan RGH, et al. Diagnostic Performance of Dedicated Axillary T2 and Diffusion-weighted MR Imaging for Nodal Staging in Breast Cancer. Radiology. 2015;275(2):345-55.

40. He N, Xie C, Wei W, Pan C, Wang W, Lv N, Wu P. A new, preoperative, MRI-based scoring system for diagnosing malignant axillary lymph nodes in women evaluated for breast cancer. Eur J Radiol. 2012;81(10):2602-12.

41. Kamitani T, Hatakenaka M, Yabuuchi H, Matsuo Y, Fujita N, Jinnouchi M, Nagao M. Detection of axillary node metastasis using diffusion-weighted MRI in breast cancer. Clin Imaging. 2013;37(1):56-61.

42. Giuliano AE, Hunt KK, Ballman KV, et al. Axillary dissection vs no axillary dissection in women with invasive breast cancer and sentinel node metastasis: a randomized clinical trial. JAMA. 2011;305(6):569-75.